

# Scanning probe microscopy applied to the study of domains and domain walls in a ferroelectric $\text{KNbO}_3$ crystal

J. CANET-FERRER<sup>1</sup>, L. MARTÍN-CARRÓN<sup>1</sup>,  
J. L. VALDÉS<sup>1</sup> and J. MARTÍNEZ-PASTOR<sup>1</sup>

<sup>1</sup>Instituto de Ciencia de los Materiales de la Universidad de Valencia, E-46071 Valencia, Spain.

A commercial Atomic Force Microscope (AFM) and a semi-home made Scanning Near-Field Optical Microscope (SNOM) have been used to characterize electrically, topographically and optically the domain walls among natural ferroelectric domains in a  $\text{KNbO}_3$  crystal. The AFM measurements have been performed with a metallic coated tip in order to detect electrostatic forces between the polarization field at the ferroelectric surface and the tip. An external electric field has also been applied between the sample surface and the tip to tune this electrostatic interaction over the atomic forces. In optical transmission images, acquired under near field conditions, we observe a clear contrast of the signal at the domain walls between  $180^\circ$  spontaneous polarization domains; while the images of the surface topography, obtained simultaneously, show a reasonably flat surface of the crystal. The scanning probe microscopy techniques used in this work are valuable tools for the investigation of ferroelectric materials and, in particular, to characterize the domain walls, without needing a either especial preparation or damage of the sample surface.

*Keywords:*  $\text{KNbO}_3$ , ferroelectric, domain-wall, SNOM and AFM

**Microscopias de barrido aplicadas al estudio de los dominios y las paredes de dominio en un cristal ferroelectrico de  $\text{KNbO}_3$ .**

Hemos utilizado un Microscopio de Fuerzas Atómicas (AFM) comercial y un Microscopio Óptico de Campo Cercano (SNOM) semi-casero para caracterizar eléctrica, óptica y topográficamente las paredes de dominio presentes entre los dominios ferroeléctricos naturales de un cristal de  $\text{KNbO}_3$ . Las medidas de AFM las hemos realizado con una punta recubierta con metal, para detectar las fuerzas electrostáticas entre los campos de polarización de la superficie ferroeléctrica y la punta. Además, hemos aplicado campos eléctricos externos entre la superficie de la muestra y la punta, de manera que se pueda variar la fuerza electrostática en relación a las fuerzas atómicas. En imágenes de transmisión óptica, bajo condiciones de campo cercano, observamos un claro contraste de la señal en las fronteras entre los dominios ferroeléctricos con polarización espontánea a  $180^\circ$ , mientras que las imágenes de topografía muestran una superficie prácticamente plana. Las técnicas de microscopía de prueba usadas en este trabajo se revelan muy valiosas para la investigación de materiales ferroeléctricos y, en particular, para la caracterización de sus dominios y paredes de dominio, puesto que no es necesario preparar ni dañar la superficie de la muestra para ser investigada.

*Palabras clave:*  $\text{KNbO}_3$ , ferroeléctrico, pared de dominio, SNOM y AFM

## 1. INTRODUCTION

Potassium niobate ( $\text{KNbO}_3$ ) belongs to the group of perovskite-type ferroelectrics of the barium titanate family. Extensive theoretical and experimental studies (1-4) have been performed on this material since the discovery of its ferroelectricity (5), because its out-standing electro-optical, nonlinear optical and photorefractive properties. In the last decade,  $\text{KNbO}_3$  (KNO) single crystal has received much attention (4, 6-8) due to the relation existent between the piezoelectric properties and the domain structures. However, many of these properties are not well understood at the nanometer scale in bulk material and thin films. Some ferroelectric crystals, for example  $\text{LiNbO}_3$  and  $\text{KNbO}_3$ , form natural periodic and quasi-periodic domain structures. Domain wall movement plays a key role in the macroscopic response. In particular, the pinning-depinning dynamics, caused by randomly distributed defects and impurities, is of great interest (9).

A variety of experimental techniques such as polarizing optical microscopy, etching, colloidal decoration, the anomalous dispersion of x-rays, Atomic Force Microscopy (AFM), scanning electron microscopy and transmission electron microscopy, have been used to study static domains (6,9). Electrostatic Force Microscopy (EFM) is a suitable technique for characterization of ferroelectric nano-domains (10). These Scanning Probe Techniques (SPM), in combination with Near Field Optical Microscopy (SNOM), are unique for characterization of domains and domain walls in ferroelectric crystals, since they provide the possibility of studying samples without either a especial preparation of the sample or damaging the surface, as demonstrated in this work. We have incorporated small modifications in a commercial AFM to be used as an EFM, in order to study a KNO single crystal sample, which exhibits natural periodic ferroelectric domains. We have also employed AFM and SNOM techniques

to complete the study of the ferroelectric domains at nano- and micro-metric scale, related to some of their basic optical properties and electrostatic behaviour.

**2. EXPERIMENTAL DETAILS**

At room temperature, KNO has an orthorhombic crystal structure with space group  $Amm_2$  and presents natural periodic ferroelectric domains with  $180^\circ$  spontaneous polarization (8). We have used a commercial AFM (Nanotec, Spain) and a non commercial SNOM to characterize electrical, topographically and optically, respectively, the domain walls in a KNO bulk crystal. The SNOM microscope is based on a quartz tuning fork sensor head and piezoelectric streper (and scanning) motors from Attocube, adapted to an AFM electronics (also from Nanotec).

The AFM measurements have been performed in both contact and non-contact modes, because the interaction depends on the tip-surface distance and also on the tip motion (11). The Nanotec piezoelectric scanner, with a scan size of  $17.5 \times 17.5 \times 3 \mu m^3$ , is the base of our sample holder. The electronic control and digital processing of the signals are carried out by the Dulcinea-electronics (Nanotec), where capabilities for Dynamic Force Control and Kelvin Probe Microscopy (EFM) are integrated. A PointProbePlus-cantilever (Nanosensors) with appropriate elastic and geometric properties ( $k = 2.8 \text{ N/m}$  and tip radius of 15 nm) has been used to obtain both contact and tapping AFM images of the same scanned area. We have employed a programmable DC Keithley 230 voltage source to externally apply a lateral electric field on the surface (about 100 V/mm). We can also add a DC bias between the tip and one of these contacts by means of the AFM electronics. The schematic drawn of this experimental setup is shown in Figure 1.

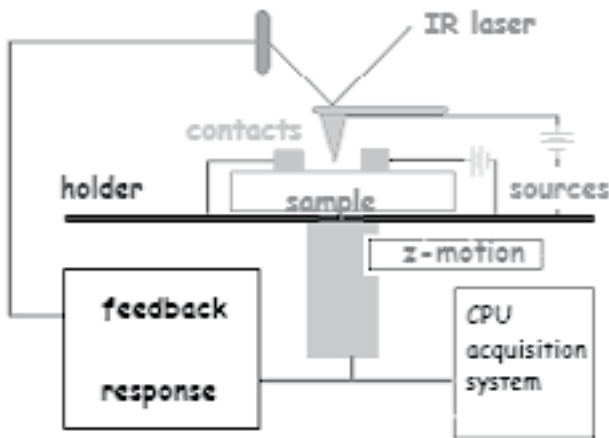


Fig. 1- Scheme of experimental setup performed to obtain electrostatic information. It is based on a typical AFM set up, where two voltage sources have been added. As can be seen in the figure, the DC voltage is applied between the tip and the surface. A lateral field can be also applied by an external voltage source. Both sources were grounded at the sample holder.

Our SNOM is capable of recording simultaneously the topography and the optical signal (transmission or reflectivity) images. The operational principles of this SNOM are similar to that of the AFM working in non-contact mode, but the

standard probe is replaced by a tip shaped and metal coated monomode optical fiber. This optical probe is mounted on a pitch-fork quartz, whose natural resonance arises at 32.7 kHz (without fiber) for vibration parallel to the sample surface. During the scan, the amplitude of such lateral vibration is kept constant by the feedback electronics (Nanotec). The feedback correction consists in a displacement of the sample along the z-axis to maintain constant the tip-sample distance, so called gap-width. The surface features are extremely correlated with this z-motion, which is used to form the topographic images. The sample surface was illuminated with a laser diode of 980 nm coupled to the free end of the optical fiber mounted on the quartz fork. The light detection was made by a Si-photodiode, whose electrical signal is connected to the AD/DA card of our AFM-electronics after pre-amplified ( $10^6$ - $10^8$ , depending on excitation) by a low-noise external current amplifier (Femto).

**3. RESULTS AND DISCUSSION**

**3.1. Electrostatic imaging with AFM.**

The electrostatic signal measured in a commercial EFM is that associated to changes on the surface potential induced by an AC modulation added to the DC bias applied between the tip and the sample surface, and typically measured by a lock-in amplifier. The electrostatic force (tip-sample) in a given point of the surface is proportional to the square of the electric potential between the tip and the sample. This potential consists in the sum of the bias applied to the tip and the difference of the potential emerging, as a result of moving the tip to a different potential area (12). In addition, the normal force presents three components due to the electrostatic interaction: a static force and two oscillating forces, whose frequencies depend on the AC modulating signal (13). We have used a more simple approach to measure local electrostatic forces, in order to obtain some more qualitative conclusions. In our experiment, a conducting probe (metal coated Si tip) has been used to observe changes on the surface potential due to the abrupt variation of the spontaneous polarization across the domain walls. We have obtained AFM images applying several combinations of voltages at the contacts. Two different effects were observed in contact mode with a conducting

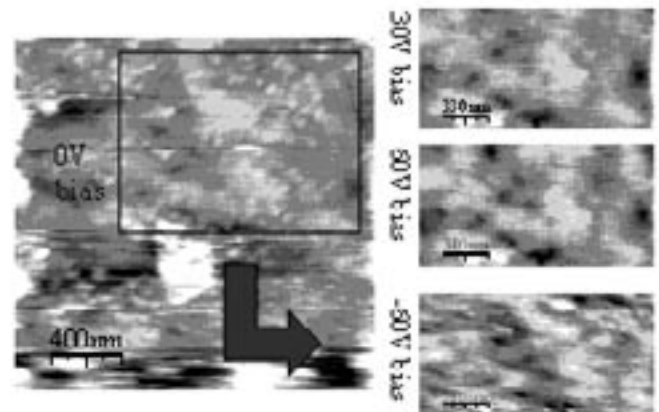


Fig. 2- Typical topography of KNO surface. Left: image obtained at 100V in lateral field and zero bias in contact mode. Right: the bias field applied of 30V, 60V and -60V from top to bottom. These contrasts are perfectly reproducible and more intense under higher electric fields, but are clearly different for both polarizations.

tip: (1) some reproducible contrasts with different features depending on the analyzed signal (topography, lateral force or normal force), and (2) a clear electrostatic contrast double-line at the domain wall. As shown below, they have been observed under different imaging conditions: without electrostatic field, applying lateral field and adding a small bias (less than 10 V) between the tip and one of the contacts.

A typical example of these contrasts is shown in Figure 2. The left panel is the topographical image, which was acquired without applying any bias to the tip, but applying 100V between the two metallic contacts made on the sample surface. The topographic resolution decreases when that lateral electric field is applied, which is attributed to an increase of the normal force component (used as the feedback signal), because of the presence of the electrostatic repulsion force. When a bias is added to the tip, also a great number of reproducible marks are observed. Their contrast increases applying this bias and their shape depends on the sign of the electric field (right side images in Figure 2).

All these measurements confirm that the measured double-line signature is related to the domain wall and the other are just electrostatic effects, which cannot be associated to the domain structure. In our opinion, these contrasts could be produced either by superficial voltages (like spontaneous polarization), charges, inductive effects and/or tip-sample capacitive effects. The last ones are interesting since they could be used to characterize ferroelectric surfaces by analysing the static component of the tip-surface interaction.

The domain walls seem also to be observed in topographic images, even without applying external fields (not shown). They were appearing like protuberances of the surface, which could be differentiated from surface wrinkles by correlating with normal force images. Given that the normal force signal coming from the domain wall is very weak, we are able to detect better domain walls by applying the lateral electric field. In this way, in Figure 3 a “dark line” (attractive force) is observed close to the domain wall by scanning along the backward direction, while a “bright line” (repulsive force) appears by scanning along the forward direction. This fact (different brightness of the two scanning directions) is the main reason why we can infer that this is an electrostatic effect as well.

### 3.2. Near-field optical microscopy Characterization.

To complete the study of ferroelectric domains in KNO, we have performed SNOM measurements. The advantage of our Near-Field Microscope is the possibility of acquiring the SNOM images, containing the optical information, and the topographical images, simultaneously. In this way, we can correlate the optical information of the sample (transmission or reflectivity) with the surface topography. Our optical (and topographic) probes reach a resolution better than 100 nm along the lateral directions and around 1 nm in the axial one. When the tip is approached close to the surface, maintaining a constant height about 15 nm, the light arrives to the detector by tunnelling this gap and going across the sample. As a result, the light reaching the Si-photodetector from each point

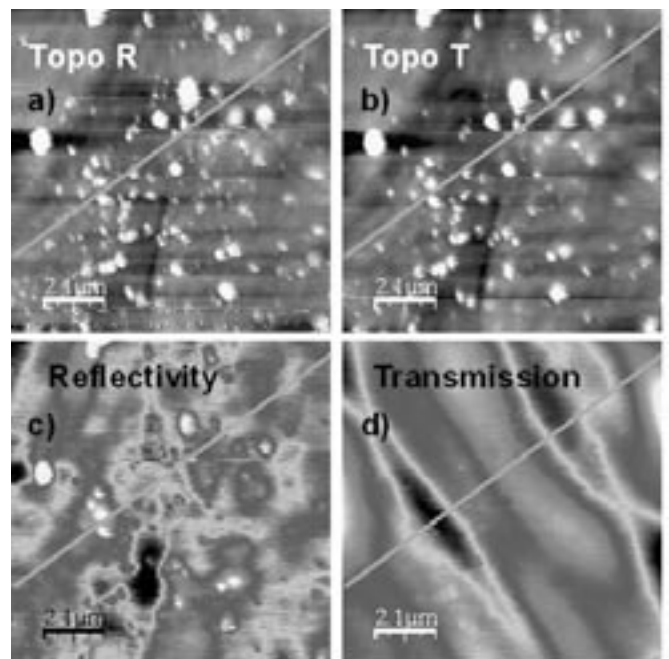


Fig. 4- (a) and (b) correspond to topography images obtained simultaneously as the optical reflectivity (c) and transmission (d) ones under near field conditions.

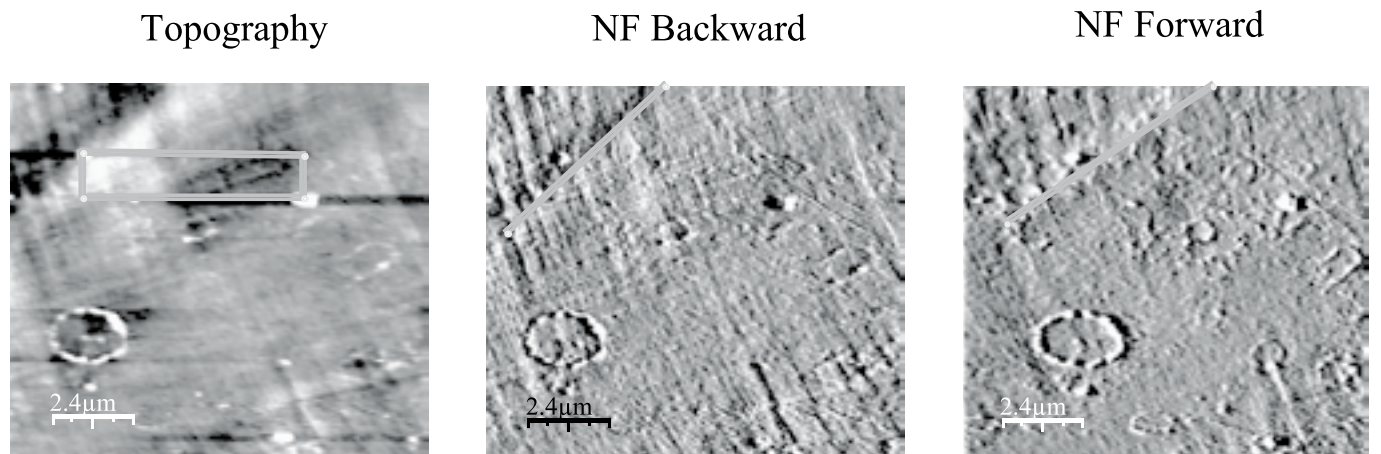


Fig. 3- Domain wall observed by electrostatic interaction. Left: topographic image of the domain wall, which appears without applying field. Middle and right: backward and forward normal force signal, which exhibit attractive or repulsive contrasts at the domain wall depending on the scanning direction.

of the sample surface will depend on the tip-surface gap and on the sample refractive index, since the evanescent fields are transformed into propagating waves by interaction between the probe and the sample in the near-field range (14). This is the reason why the transmission signal usually contains the optical information as well as the topographic one (15).

Figure 4 shows the SNOM images (transmission and reflectivity) of the same surface region of the sample. We have also included the topography belonging to these images to check that we are scanning the same region (top images in Figure 4). At first sight, we can see that the reflectivity image mostly reproduces the topography of the sample (plus a high number of dust particles), which is not the case for the transmission image. In this image we observe clear contrasts, which are attributed to the change of the refractive index produced at the domain walls (16). The correlation between optical and mechanical information is considered one of the key issues in SNOM microscopy, necessary to interpret correctly optical images. The surface roughness is usually reproduced in SNOM images and optical information sometimes becomes a (less intense) second order effect. In addition, topographic artefacts can be sometimes observed, due to inappropriate feedback response, sample flatness and other effects (14-15). This is not the case in the SNOM transmission images measured in KNO<sub>3</sub>, which exhibit a clear contrast associated to the domain walls between 180° spontaneous polarization domains, and signal changes induced by surface protuberances (dust particles) become negligible.

In Figure 5 we present some profiles extracted from the images in Figure 4. We measure changes in the transmitted light larger than 30 mV [see Fig. 5(b)] over an average value of around 2 V, that is, the contrast in the transmittance,  $\Delta T/T$ , is larger than 1 %, which corresponds to a contrast in the refractive index,  $\Delta n/n$ , larger than 2%. The contrast for  $n$  has been estimated considering a simple expression that relates the optical transmission with the refractive index for normal incidence conditions,

$$\frac{(n+1)dSignal}{(n-1)Signal} = -\frac{(n+1)dT}{(n-1)T} = \frac{dn}{n}$$

thus it should be considered as an approximation. These contrasts appear without having topographic signal, that is, the topographic images obtained simultaneously as the optical ones show a reasonably flat surface [see Figs. 5(a) and (c)], except sharp peaks associated to the dust particles. On the contrary, the topography of the sample is mainly determining the reflectivity image shown in Figure 4 (including similar sharp peaks as in topography, associated to the dust particles). Furthermore, when we analyse in more detail the reflectivity profiles [like that shown in Fig. 5(d)], we observe an extra modulation associated to an optical contrast, of course weaker than that observed in transmission. This optical contrast can be separated from that corresponding to the topographic features. The fact that this modulation is practically inverse to that observed in the transmission profiles (maxima in transmission correspond to minima in reflectivity) confirm that the optical contrast in the domain-wall is produced by a change in the refractive index. Finally, we can extract from the profiles that the average separation between domain walls is around 1500 nm and their typical width 700 nm, approximately, which can be the origin of the strong second harmonic generation typically observed in this kind of samples at room temperature.

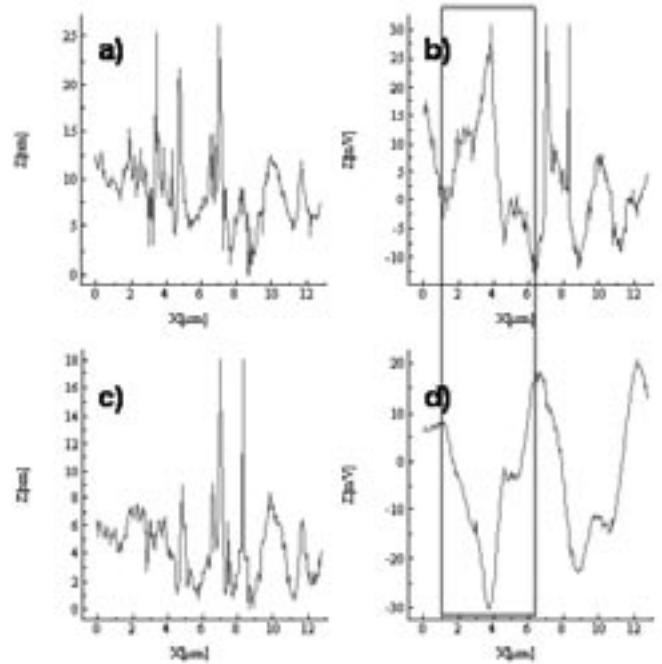


Fig. 5- Profiles (a) to (d) are extracted from the corresponding images in Fig. 4.

#### 4. CONCLUSIONS

In contact mode AFM measurements, a coulombian repulsion to the tip can be produced by applying a lateral electric field. On the one hand, this repulsion explains the lost of resolution in spite of the enhancement of the contrasts in the topographic images. On the other hand, some domain walls were observed without applying field, which appeared like a protrusion of the surface. They could be also observed as contrasts in normal force images under electric field, indicating that they are not merely topographic effects. In the SNOM transmission images we observe a clear contrast of the signal at the domain walls between 180° spontaneous polarization domains, which is of the order of 1 % in the optical transmittance (there are more and less intense throughout the surface) and corresponds to a contrast in the refractive index of around a 2%. These contrasts appear without having topographic signal. We also determined the average separation between domain walls to be around 1500 nm and their typical width 700 nm, approximately. These SPM techniques are very useful for characterization of domains and domain walls in ferroelectric materials in the nanometre scale. Both of them provide the possibility of studying samples without a special preparation of the surface (chemical selective etching, for example), as done to observe periodic domain structures by traditional optical microscopy.

#### ACKNOWLEDGEMENTS

We want to acknowledge C. Zaldo for providing the sample.

We acknowledge the "Ministerio de Educación y Ciencia" for financial support under contract MAT2002-04603-C05-02 and L. Martín-Carrón wants also to acknowledge the "Ministerio de Educación y Ciencia" for financial support under contract program "Juan de la Cierva".

## REFERENCES

1. M. Zgonik, R. Schlessler, I. Biaggio, E. Voit, J. Tscherry and P. Gunter. "Materials constants of  $\text{KNbO}_3$  relevant for electro-and acousto-optics". *J. Appl. Phys.* 74, 1287-1297 (1993).
2. A.V. Postnikov, T. Neumann, G. Borstel and M. Methfessel. "Ferroelectric structure of  $\text{KNbO}_3$  and  $\text{KTaO}_3$  from first-principles calculations". *Phys. Rev. B.* 48, 5910-5918 (1993).
3. R.D. King-Smith, D. Vanderbilt. "First-principles investigation of ferroelectricity in perovskite compounds". *Phys. Rev. B.* 49, 5828-5844 (1994)
4. C. Duan, W.N. Mei, J. Liu and J.R. Hardy. "First-principles study on the optical properties of  $\text{KNbO}_3$ ". *J. Phys.: Condens. Matter.* 13, 8189-8195 (2001).
5. B.T. Matthias. "New ferroelectric crystals". *Phys. Rev.* 75, 1771 (1949)
6. R. Lüthi, H. Haefke, K.P. Meyer, E. Meyer, L. Howald and H.J. Güntherodt. "Surface and domain structures of ferroelectric crystals studied with scanning force microscopy". *J. Appl. Phys.* 74, 7461-7471 (1993).
7. H. Bluhm, U.D. Schwarz and R. Wiesendanger. "Origin of the ferroelectric domain contrast observed in lateral force microscopy" *Phys. Rev. B.* 57, 161-169 (1998).
8. V.Yu Topolov "Domain wall displacements and piezoelectric activity of  $\text{KNbO}_3$  single crystals" *J. Phys.: Condens. Matter* 15, 561 (2003)
9. T. J. Yang et al. "Direct observation of pinning and bowing of a single ferroelectric domain wall". *Phys. Rev. Lett.* 82, 4106-4109 (1999); and references therein.
10. M. Labardi, V. Likodimos and M. Allegrini. "Force-microscopy contrast mechanisms in ferroelectric domain imaging". *Phys. Rev. B.* 61, 14390-14398 (2000)
11. P. Shivprasad et al. "Study of the electrostatic force between a conducting tip in proximity with a metallic surface: theory and experiment". *J. of Appl. Phys.* 88, 6940-6942 (2000)
12. U. Zerweck, C. Loppacher, T. Otto, S. Granfström and L.M. Eng. "Accuracy and resolution limits of Kelvin probe force microscopy". *Phys. Rev. B.* 71, 125424 (2005).
13. R. Rousier, P. Vairac and B. Cretin. "Measurement of the contact potential difference with an electrostatic force microscope". *Eur. J. Phys.* 22, 657-662 (2001)
14. S. Wang and J.M. Siqueiros. "Influence of the sample-probe coupling on the resolution of transmitted near-field optical image". *Opt. Lasers Eng.* 31, 517- (1999).
15. B. Hecht, H. Bielefeldt, Y. Inoute, D. W. Pohl and L. Novotny. "Facts and artefacts in near-field optical microscopy". *J. Appl. Phys.* 81, 2492-2498 (1997).
16. H. Chaib, T. Otto, and L.M. Eng. "Theoretical study of ferroelectric and optical properties in the  $180^\circ$  ferroelectric domain wall of tetragonal  $\text{BaTiO}_3$ ". *Phys. Stat. Sol.* 233, 250-262 (2002).

Recibido: 15.07.05

Aceptado: 31.01.06

